Interleaved Soft-Switching Buck Converter with Coupled Inductors

Cheng-Tao Tsai and Chih-Lung Shen

Abstract—**This paper presents an interleaved soft-switching buck converter with coupled inductors to extend duty ratio for high step-down voltage applications. In the proposed converter, a single-capacitor turn-off snubber is introduced to limit rising rate of active switches to reduce turn-off loss. To handle the energy trapped in the leakage inductance of the coupled inductors, simple passive-clamp circuits are added to the proposed converter, which can effectively recycle the energy and suppress voltage spike. To highlight the merits of the proposed converter, its performance indexes, such as voltage gain function and component stresses, are analyzed and compared with those of the conventional interleaved buck converter. In this study, the prototype of the proposed converter, input voltage of 150-200 V_{dc}, output voltage of 12 V_{dc}, and full load power of 240 W has been implemented and verified, from which experimental results have shown that 85% conversion efficiency can be achieved at the full load condition.**

Index Terms—**Interleaved, soft-switching, coupled inductors, leakage inductance, passive-clamp circuits.**

I. Introduction

Interleaved buck converter (IBC) with a single- capacitor turn-off snubber was proposed to achieve soft-switching function [1], as shown in Fig. 1. Although it can reduce switching loss and output current ripple, its efficiency is not attracted at high step-down voltage applications. The reason behind is that it suffers from extremely low duty ratio and high component stress. For example, when input voltage is 156 V_{dc} and output voltage is 12 V_{dc}, its duty ratio is only 0.077. Additionally, reverse-recovery problems of the free-wheeling diodes become severe issues when the input voltage goes beyond a high level and there are no proper Schottky diodes available. The reverse-recovery current of the free-wheeling diodes has detrimental effects on the performance of the IBC. When the IBC is operated in CCM, high switching loss resulting from the reverse-recovery current dramatically deteriorates the thermal condition of the free-wheeling diodes. These drawbacks limit the soft-switching IBC from high step-down voltage applications.

To overcome the drawbacks, utilizing coupled inductors is a solution [2]-[5]. It has a simpler winding structure, and always transfers power to the output through the primary winding, reducing peak primary winding current. Thus, a converter with a coupled inductor is relatively attractive because the converter presents an extendable duty ratio and low diode voltage stress. Fig. 2 shows the proposed soft-switching IBC with coupled inductors. Although it can yield high step-down voltage gain, the leakage inductance of the coupled inductors resonates with the parasitic capacitance of the active switches, which not only increases the voltage stress of the active switches, but induces significant loss. To handle the energy trapped in the leakage inductance, a dissipative snubber could be used, but it results in lower efficiency. Simple passive-clamp circuits are added to the proposed interleaved coupled-buck converter (ICBC), as shown in Fig. 3, which can effectively recycle the leakage energy and suppress voltage spike [6]. With the proposed converter, conversion efficiency therefore can be improved significantly.

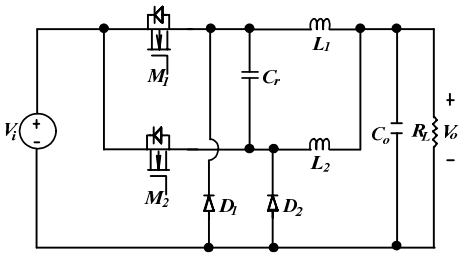

Fig. 1. Topology of IBC with a single-capacitor turn-off snubber.

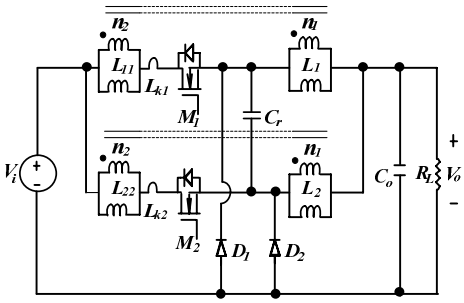

Fig. 2. Topology of ICBC with a single-capacitor turn-off snubber.

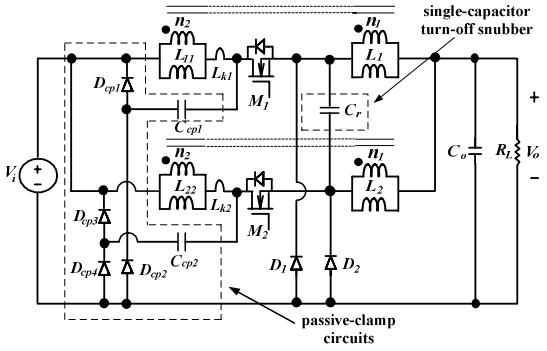

Fig. 3. Topology of ICBC with passive-clamp circuits.

II. Operational Principle and Feature Analysis

As shown in Fig. 3, the proposed ICBC consists of two sets of coupled-buck converters, two sets of passive-clamp circuits and a single-capacitor turn-off snubber. The driving signals, current and voltage waveforms of its key components are shown in Fig. 4. In Fig. 3, each coupled inductor can be replaced with an equivalent transformer and two magnetizing inductors in this section.

Cheng-Tao Tsai received the Ph.D. degree from National Chung Cheng University, Chia-Yi, Taiwan. He is now with BESTEC Power Electronics Co., Ltd., Taipei, Taiwan(e-mail: swn28589@yahoo.com.tw).

Chih-Lung Shen is with the Department of Electronic Engineering, National Kaohsiung First University of Science and Technology, Yuanchau, Kaohsiung, Taiwan (e-mail: clshen@ccms.nkfust.edu.tw; phone: +886-7-6011000 ext. 2515; fax: +886-7-6011386).

978-1-4244-1888-6/08/$25.00 © 2008 IEEE

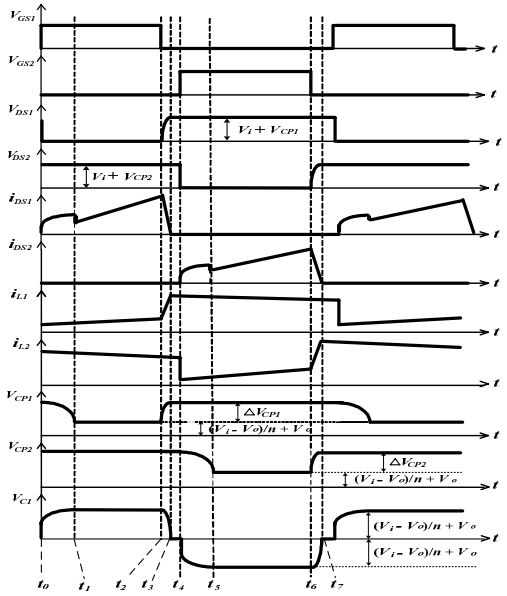

Fig. 4. Key waveforms of the ICBC with passive-clamp circuits.

A. Operational Principle

To simplify the description of the operational modes, the following assumptions are made.

1) Capacitance of C_o, C_{CP1} and C_{CP2} is large enough so that the voltages across them are constant over a switching period.
2) All of the switching devices, MOSFETs and diodes, are ideal.

Based on the above assumptions, operation of the proposed converter over one switching cycle can be divided into seven modes. Fig. 5 shows the topological modes of the proposed converter over a switching cycle. Operation of the converter is explained mode by mode as follows:

***Mode 1* [Fig. 5(a), $t_0 \le t < t_1$]:**

This mode begins when M_1 starts conducting at t_0. Coupled inductors L_{l1} and L_1 are linearly charged, and inductor current i_{L1} flowing through the path of V_o-V_i-L_{l1}-L_{k1}-M_1-L_1 linearly increases. At the same time, clamp capacitor C_{CP1} is discharged and snubber capacitor C_r begins resonating with leakage inductance L_{k1}. During this interval, switch M_2, clamp diodes D_{CP1}, D_{CP3} and D_{CP4}, and free-wheeling diode D_1 are in the off states. The energy stored in inductor L_{22} will be released to the load through coupled inductor L_2, and inductor current i_{L2} flowing through the path of V_o-D_2 is decreased. The coupled inductor currents i_{L1} and i_{L2} can be expressed as follows:

$$i_{L1}(t) = \frac{V_i - V_o}{n^2 L_1} \times (t - t_0) + i_{L1}(t_0), \tag{1}$$

and

$$i_{L2}(t) = \frac{V_o}{nL_2} \times (t - t_0) + i_{L2}(t_0), \tag{2}$$

where V_i and V_o are input voltage and output voltage, and n is the turns ratio of the coupled inductors L_1 and L_{l1} or L_2 and L_{22}.

***Mode 2* [Fig. 5(b), $t_1 \le t < t_2$]:**

At time t_1, the clamp capacitor C_{CP1} is discharged to the steady-state voltage value and snubber capacitor C_r is completely charged. The clamp capacitor and snubber capacitor voltages can be expressed as follows:

$$V_{CP1} = V_{Cr} = \frac{(V_i - V_o)}{n} + V_o. \tag{3}$$

***Mode 3* [Fig. 5(c), $t_2 \le t < t_3$]:**

At time t_2, switch M_1 is turned off, and switch M_2, clamp capacitors D_{CP3} and D_{CP4} as well as free-wheeling diode D_1 still stay in the off states. Snubber capacitor C_r begins discharging, and the energy trapped in leakage inductance L_{k1} is transferred to clamp capacitor C_{CP1}. If C_{CP1} is large enough and the increased voltage across C_{CP1} is relatively small, its value is about

$$\Delta V_{CP1} = \frac{L_{k1} \times i_{DS1}^2}{2C_{CP1} \times V_{CP1}}. \tag{4}$$

Thus, the total voltage of C_{CP1} can be expressed as follows:

$$V_{CP1(total)} = \frac{(V_i - V_o)}{n} + V_o + \Delta V_{CP1}. \tag{5}$$

***Mode 4* [Fig. 5(d), $t_3 \le t < t_4$]:**

In this mode, as the voltage of snubber capacitor C_r drops to zero, free-wheeling diode D_1 is conducting. The energy stored in inductor L_{l1} will be released to the load through coupled inductor L_1, and inductor current i_{L1} flowing through the path of V_o-D_1 is decreased. Coupled inductor currents i_{L1} and i_{L2} can be expressed as follows:

$$i_{L1}(t) = \frac{V_o}{nL_1} \times (t - t_3) + i_{L1}(t_3), \tag{6}$$

and

$$i_{L2}(t) = \frac{V_o}{nL_2} \times (t - t_3) + i_{L2}(t_3). \tag{7}$$

***Mode 5* [Fig. 5(e), $t_4 \le t < t_5$]:**

At time t_4, switch M_2 is conducting, coupled inductors L_{22} and L_2 are linearly charged, and inductor current i_{L2} flowing through the path of V_o-V_i-L_{22}-L_{k2}-M_2-L_2 linearly increases. Meanwhile, clamp capacitor C_{CP2} is discharged and snubber capacitor C_r begins resonating with leakage inductance L_{k2}. During this interval, switch M_1, clamp diodes D_{CP1}, D_{CP2} and D_{CP3}, and free-wheeling diode D_2 are in the off states. The energy stored in inductor L_{22} will continue releasing to the load through coupled inductor L_2. Coupled inductor currents i_{L1} and i_{L2} can be expressed as follows:

$$i_{L1}(t) = \frac{V_o}{nL_1} \times (t - t_4) + i_{L2}(t_4), \tag{8}$$

and

$$i_{L2}(t) = \frac{V_i - V_o}{n^2 L_2} \times (t - t_4) + i_{L1}(t_4), \tag{9}$$

***Mode 6* [Fig.5(f), $t_5 \le t < t_6$]:**

At time t_6, clamp capacitor C_{CP2} is discharged to the steady-state voltage value and snubber capacitor C_r is completely charged. The clamp capacitor and snubber capacitor voltages can be expressed as follows:

$$V_{CP2} = V_{C2} = \frac{(V_i - V_o)}{n} + V_o. \tag{10}$$

***Mode 7* [Fig. 5(g), $t_6 \le t < t_7$]:**

At time t_6, switch M_2 is turned off, and switch M_1, clamp capacitors D_{CP1}, D_{CP2} and D_{CP4} as well as free-wheeling diode D_2 still stay in the off states. Snubber capacitor C_r begins discharging, and the energy trapped in leakage inductance L_{k2} is transferred to clamp capacitor C_{CP2}. If C_{CP2} is large enough and the increased voltage across C_{CP2} is relatively small, its value is about

$$\Delta V_{CP2} = \frac{L_{k2} \times i_{DS2}^2}{2C_{CP2} \times V_{CP2}}. \tag{11}$$

Thus, the total voltage of C_{CP2} can be expressed as follows:

$$V_{CP2(total)} = \frac{(V_i - V_o)}{n} + V_o + \Delta V_{CP2}. \tag{12}$$

When switch M_1 starts conducting again at the end of Mode 7, the converter operation over one switching cycle is completed.

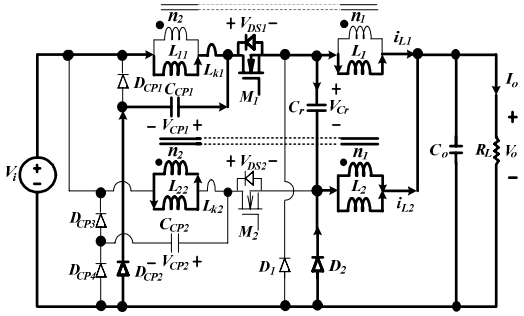

(a) Mode 1.

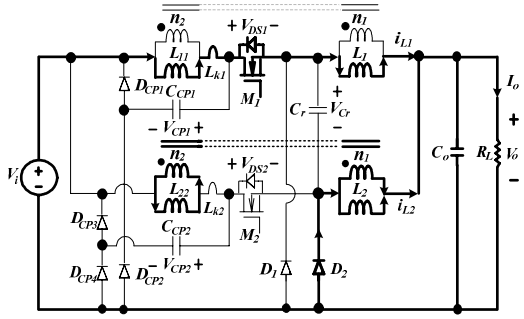

(b) Mode 2.

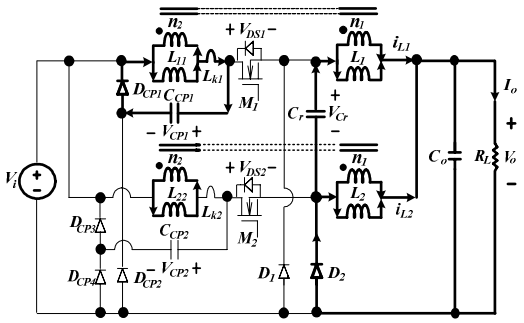

(c) Mode 3.

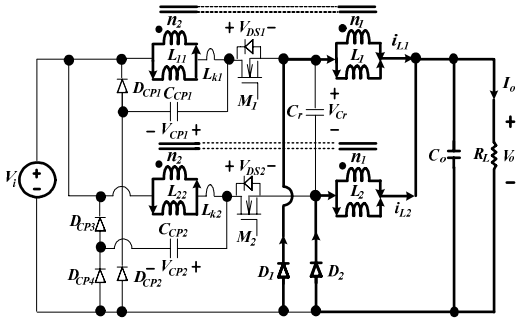

(d) Mode 4.

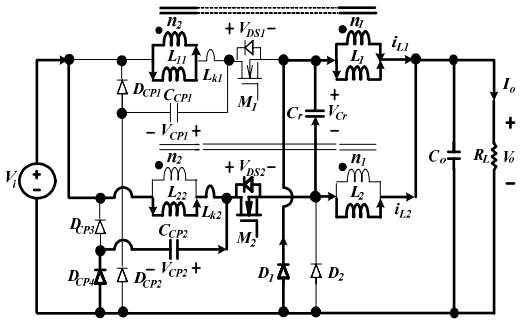

(e) Mode 5.

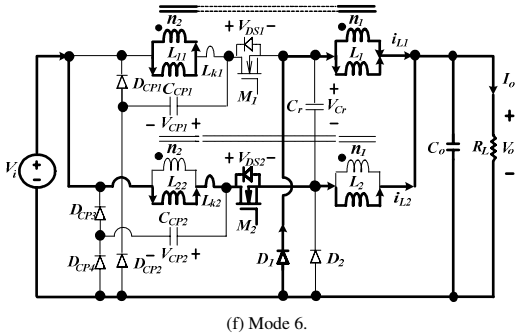

(f) Mode 6.

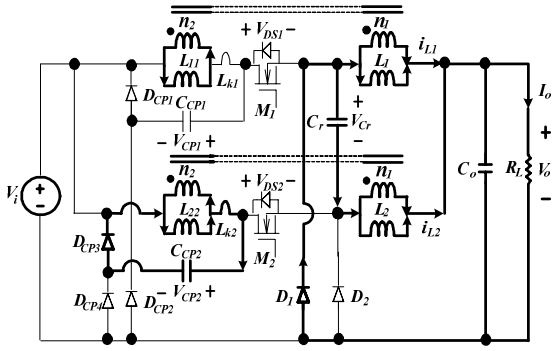

(g) Mode 7.

Fig. 5. Equivalent circuit modes of the ICBC with passive-clamp circuits operating over one switching cycle.

B. References

The proposed ICBC can extend duty ratio of the active switches and reduce component stress. This section describes the feature analysis for the proposed ICBC. The feature analysis includes voltage gain, duty ratio, and voltage stresses of diode and active switch.

1) Voltage Gain and Duty Ratio

From the key waveforms of the converter shown in Fig. 4 and by applying the volt-second balance law, the voltage gain and duty ratio can be derived as

$$\frac{V_o}{V_i} = \frac{D}{D + n(1-D)}, (n \neq 0), \tag{13}$$

and

$$D = \frac{nV_o}{V_i + nV_o - V_o}, (D < 0.5), \tag{14}$$

where D is the duty ratio of the active switch.

For example, input voltage V_i = 150-250 V_{dc} and output voltage V_o = 12 V_{dc} are considered. From (13) and (14), we can sketch a set of curves showing the relationship between duty ratio D and voltage gain of V_o/V_i for different values of turns ratio n, as illustrated in Fig 6.

2) Voltage Stresses of Diode and Active Switch

At Mode 1, free-wheeling diode D_1 and active switch M_2 stay in the off state, while D_2 and M_1 are conducting. At Mode 5, the states of D_1 and D_2 as well as M_1 and M_2 are exchanged. Their voltage stress can be derived as

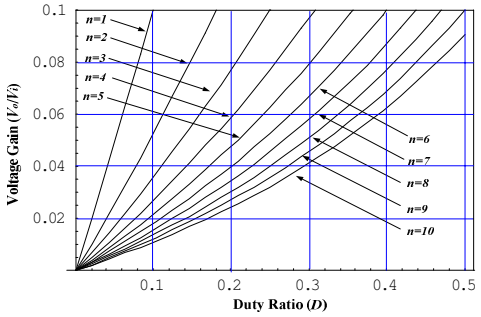

Fig. 6. Plots of V_o/V_i versus duty ratio D.

$$V_D = \frac{(V_i - V_o)}{n} + V_o, \tag{15}$$

and

$$V_{DS} = V_i + (n-1)V_o, \tag{16}$$

where V_D is the voltage stress of the diode and V_{DS} is the voltage stress of the active switch. From (15) and (16), we can sketch a set of curves showing the free-wheeling diode and active switch versus different values of turns ratio n, respectively, as shown in Fig. 7 and Fig. 8.

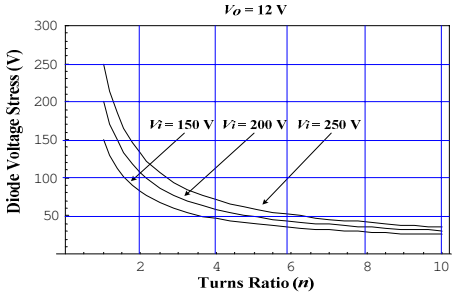

Fig. 7. Plots of diode voltage stress versus turns ratio n of the coupled inductor.

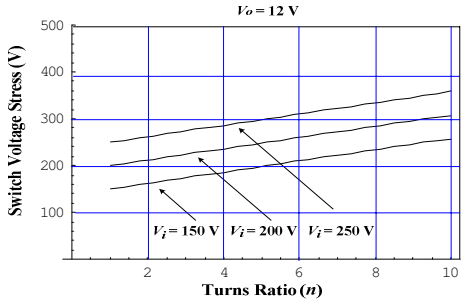

Fig. 8. Plots of switch voltage stress versus turns ratio n of the coupled inductor.

To objectively judge the merits of the proposed converter, performance comparison between the proposed converter and the IBC is shown in Fig. 9. From these plots, it can be seen that the proposed ICBC yields higher duty ratio and lower diode voltage stress over the IBC, but the proposed ICBC has higher switch voltage stress. This drawback can be overcome by a MOSFET with low $R_{ds(on)}$.

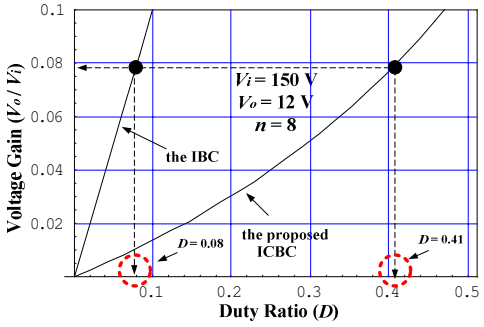

(a)

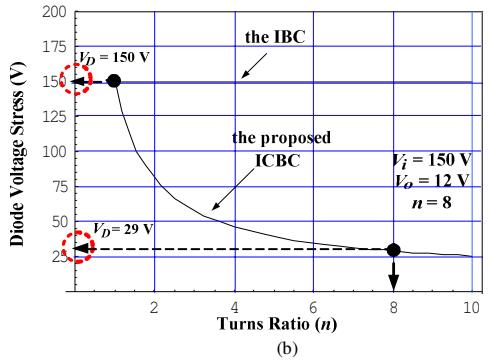

(b)

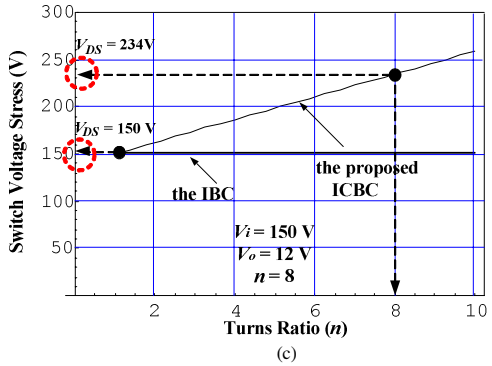

(c)

Fig. 9. Performance comparison between the ICBC and the IBC: (a) duty ratio, (b) voltage stress of the diode and (c) voltage stress of the active switch.

III. Experimental Results

To verify the operation and evaluate the performance of the proposed ICBC, the key component values of the experimental converter are shown in Fig. 10.

Fig. 11 shows simulated and experimental current waveforms of the coupled inductors. Fig. 12 shows simulated and experimental waveforms of the active switch voltage and current. It can be seen that there is not any spike voltage across the active switch. Fig. 13(a) shows expanded waveforms of the active switch voltage and current at turn-on transition, from which it can be seen that the active switch has large turn-on loss. The turn-on loss is due to the proposed converter being operated in a hard-switching manner during turn-on transition. Fig. 13(b) shows expanded waveforms of the active switch voltage and current at turn-off transition, from which it can be seen that the turn-off loss is reduced due to with a single-capacitor snuber. Fig. 14 shows measured waveforms of the free-wheeling diode voltage and current. It can be seen that the free-wheeling diode has low voltage stress and low reverse-recovery loss. Fig. 15 shows the efficiency measurements of the proposed ICBC, which can reach 85% under full load condition.

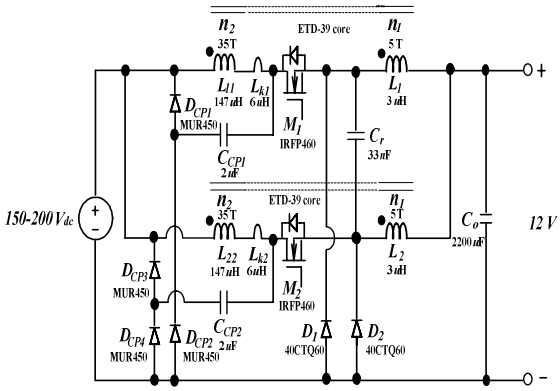

Fig. 10. Experimental circuit of the ICBC with passive-clamp circuits.

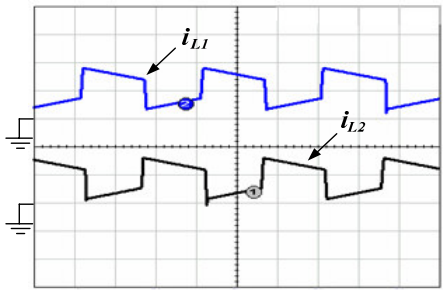

(i_{L1}: 10A/div, i_{L2}: 10A/div, Time: 5μs/div)
(a)

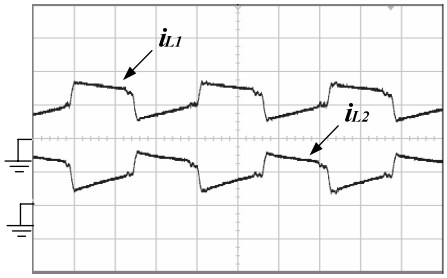

(i_{L1}: 10A/div, i_{L2}: 10A/div, Time: 5μs/div)
(b)

Fig. 11. Waveforms of inductor currents i_{L1} and i_{L2}: (a)simulated results, (b) experimental results.

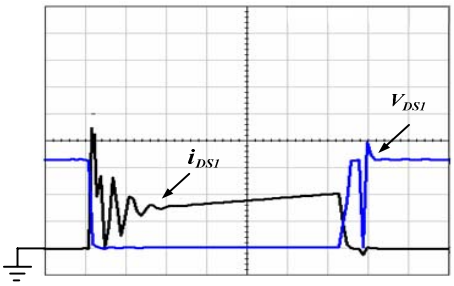

(V_{DS1}: 100V/div, i_{DS1}: 5A/div, Time: 1μs/div)
(a)

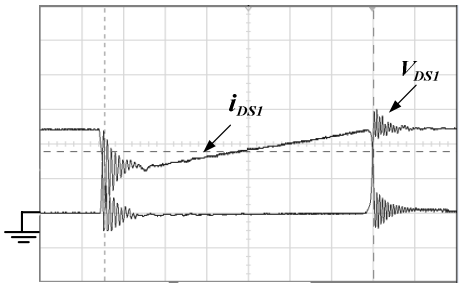

(V_{DS1}: 100V/div, i_{DS1}: 5A/div, Time: 1μs/div)
(b)

Fig. 12. Voltage and current waveforms of active switches: (a) simulated results, (b) experimental results.

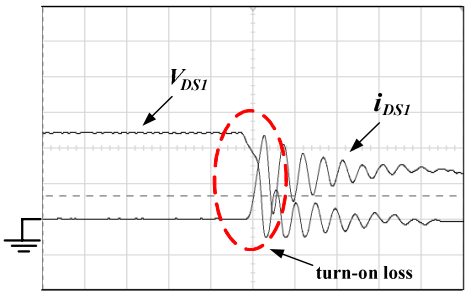

(V_{DS1}: 100 V/div, i_{DS1}: 5 A/div, Time: 200 *n*s/div)
(a)

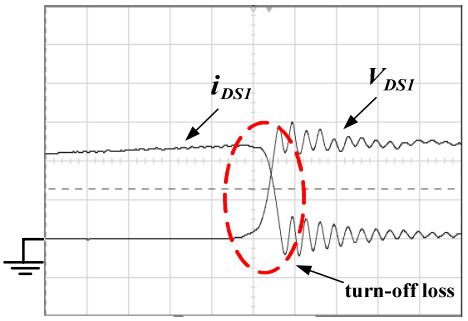

(V_{DS1}: 100 V/div, i_{DS1}: 5 A/div, Time: 200 *n*s/div)
(b)

Fig 13. Expanded voltage and current waveforms of active switches: (a) turn-on loss, and (b) turn-off loss.

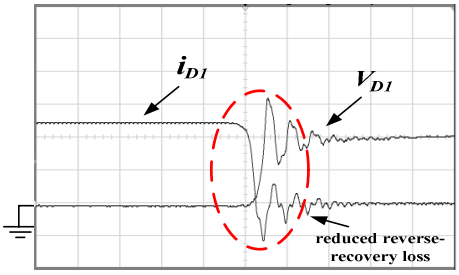

(V_{D1}: 20 V/div, i_{D1}: 10 A/div, Time: 200 *n*s/div)

Fig 14. Measured voltage and current waveforms of the free-wheeling diodes.

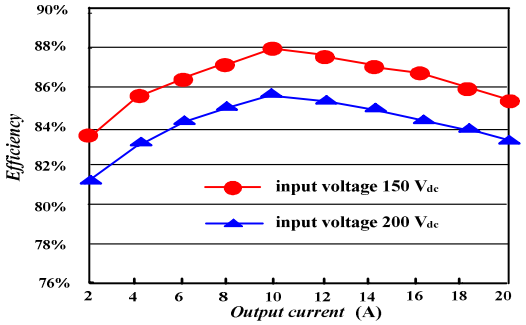

Fig 15. Plots of efficiency versus output current for the ICBC with passive-clamp circuits with different input voltages.

IV. Conclusions

In this chapter, the proposed soft-switching ICBC has been analyzed and implemented. The proposed converter with coupled inductors can extend duty ratio of the active switch and reduce component stress. In addition, by utilizing the passive-clamp circuits, the energy trapped in the leakage inductance can be recovered and voltage spike can be suppressed effectively. Experimental results have verified that the proposed ICBC can achieve high efficiency over a wide load range. It is relatively suitable for high step-down voltage applications.

References

[1] Y.-M. Chen, *et al.*, "Interleaved Buck Converters with a Single-Capacitor Turn-Off Snubber," *IEEE Trans. on Aerospace and Electronic System*, Vol. 40, No. 3, July 2004, pp. 954-967.

[2] R. Martinelli and C. Ashley, "Coupled Inductor Boost Converter with Input and Output Ripple Cancellation," *Proceeding of the Applied Power Electronics Conference*, 1991, pp. 567–572.

[3] K. Yao, *et al.*, "Tapped Inductor Buck Converters with a Lossless Clamp Circuit," *Proceedings of the Applied Power Electronics Conference*, Vol. 2, 2002, pp. 693–698.

[4] R. P. Lethellier, "Buck Converter with Inductive Turn Ratio Optimization," US Patent Number 6094038, 2000.

[5] P. Xu, J. Wei and F. C. Lee, "The Active-Clamp Couple-Buck Converter-A Novel High Efficiency Voltage Regulator Module," *Proceedings of the Applied Power Electronics Conference*, Vol. 1, 2001, pp. 252-257.

[6] K. Yao, *et al.*, "Tapped-Inductor Buck Converter for High-Step-Down DC-DC Conversion," *IEEE Trans. on Power Electronics*, Vol. 20, No. 4, 2005, pp. 775-780.